Radiotracer Diffusion and Ionic Conduction in a PEO-NaI Polymer Electrolyte

N. A. Stolwijk* and Sh. Obeidi

Institute of Materials Physics and Sonderforschungsbereich 458, University of Münster, Wilhelm-Klemm-Strasse 10, D-48149 Münster, Germany

(Received 13 February 2004; published 14 September 2004)

We studied ion transport in amorphous $PEO_{30}NaI$ consisting of poly(ethylene oxide) and sodium iodide in a Na-to-O ratio of 30. Diffusion coefficients of the radiotracers ^{22}Na and ^{125}I were measured for temperatures between 67 and 180 °C and compared with the overall charge diffusivity deduced from dc conductivity data. To explain the observed discrepancy between the sum of the tracer diffusivities and the charge diffusivity we propose a detailed model which is based on the formation of neutral ion pairs. Evaluating simultaneously all experimental data within this model yields not only the true diffusion coefficient of all individual species but also the ion-pairing reaction constant as a function of temperature.

DOI: 10.1103/PhysRevLett.93.125901 PACS numbers: 66.10.–x, 66.30.Hs

Over the past decades polymer electrolytes have attracted much attention because of their promising technological application as an ion-conducting medium in solid-state batteries and fuel cells. However, despite numerous studies related to ionic transport in these electrolytes the understanding of the migration mechanism is still far from being complete. A major reason for this unsatisfactory state-of-the-art may be that most studies on ion motion relied on dc conductivity measurements which yield only the net macroscopic effect of all charged mobile species. Only a few publications in this field report the use of ion-specific techniques by which the diffusion properties of cations and anions can be determined individually. One such technique is pulsed-field-gradient nuclear magnetic resonance (PFG-NMR; see, e.g., Ref. [1]). Another powerful ion-specific method, i.e., radiotracer diffusion, was employed only on a very small number of polymer-salt systems [2,3].

Both the PFG-NMR and the radiotracer experiments have provided valuable data such as, e.g., unambiguous evidence that the anion is moving at least as fast as the cation in all systems examined [1–3]. However, the detailed information disclosed by the ion-specific methods also raised new questions. For instance, why do cations and anions exhibit different slopes or curvatures in Arrhenius plots of the diffusivity? And related to this, how can the pronounced temperature dependence of the cation transference number be explained? Another common observation is that the sum of the individual ionic tracer diffusion coefficients tends to exceed the charge diffusivity D_σ deduced from dc conductivity σ_{dc} via the Nernst-Einstein equation. This phenomenon has been attributed to the occurrence of neutral ion pairs [4]. However, a satisfactory theoretical description of the conductivity-diffusivity discrepancy is still missing.

In this Letter we compare for $PEO_{30}NaI$, consisting of poly(ethylene oxide) (PEO) and sodium iodide, the diffusivity of ^{22}Na and ^{125}I with the overall ionic conductivity over a wide temperature range. It is shown that the quantitative evaluation of all data in terms of single ions and neutral ion pairs is able to solve the questions mentioned above.

PEO with a molecular weight of 8×10^6 (Aldrich) and NaI were dried under dynamic vacuum at an elevated temperature. Proper amounts of both components, adjusted to a O-to-Na ratio of 30, were dissolved in dry acetonitrile. After vacuum evaporation of the solvent, differential scanning calorimetry showed a single peak near 66 °C which reflects the melting of PEO. Samples were prepared by hot pressing in cylindrical Teflon molds under dry nitrogen atmosphere in a glove box. The radiotracers ^{22}Na and ^{125}I, commercially supplied as aqueous solutions, were dried and subsequently dissolved in acetonitrile. After addition of gel-like $PEO_{30}NaI$ (containing acetonitrile) the solution was cast onto an inert support and then subjected to prolonged solvent evaporation. The radioactive films produced in this way were of closely similar composition as the samples and thus suitable as diffusion-source material. In fact, the ratio of radioactive-to-natural isotopes in these films was less than $\sim 10^{-4}$ for either ionic species. Samples with one or more source-film pieces on top of one face were diffusion annealed between 67 and 180 °C in an oil-bath thermostat using suitable encapsulants, and subsequently quenched in water. Following microtome sectioning in a cold chamber, counting of the sections' radioactivity was performed by standard techniques. The dc conductivity of $PEO_{30}NaI$ was determined by means of frequency-dependent impedance analysis using stainless-steel electrodes in a temperature-controlled measuring cell operated under flowing nitrogen.

Figure 1 shows a typical depth profile of ^{22}Na and ^{125}I which originated from simultaneous diffusion of both isotopes into the same sample for 1 h at 150 °C. The two profiles are well fitted by the Gaussian function (solid lines), thus providing reliable data for the tracer diffu-

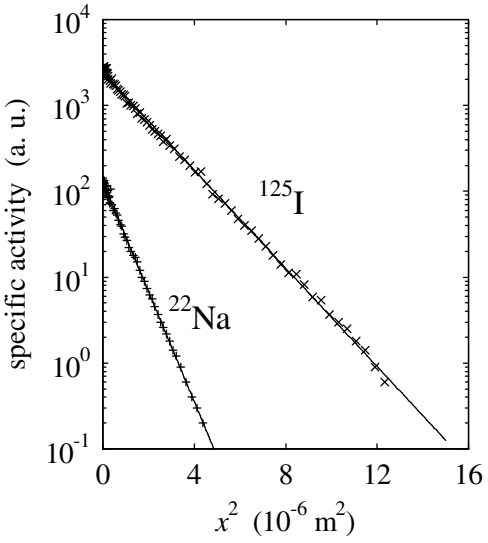

FIG. 1. Depth (x) profiles of ^{22}Na and ^{125}I in $PEO_{30}NaI$ resulting from simultaneous diffusion for 1.0 h at 150 °C. Solid lines: fits of the Gaussian function.

sivity of Na and I. In several cases complementary error function profiles were observed, which points to variations in boundary conditions related to the strength of the radioactive source. Both Gaussian and erfc-type profiles, however, reveal that the diffusion coefficient is independent of depth, which provides evidence for the homogeneity of our samples. Tracer diffusivities D^*_{Na} and D^*_I resulting from either simultaneous or separate diffusion of ^{22}Na and ^{125}I are mutually consistent. They are displayed in Fig. 2 as a function of temperature. Although in this Arrhenius plot both sets of data exhibit a fairly linear behavior, they are even better described by the slightly curved solid lines emerging from the model outlined below. Figure 2 also shows charge diffusivity data D_σ which were obtained from measurements of the dc conductivity σ_{dc} during several heating-up and cooling-down cycles. D_σ exhibits a strong downward curvature, characteristic of Vogel-Tamann-Fulcher (VTF) behavior, and falls below the sum of D^*_{Na} and D^*_I (dashed line in Fig. 2), the more so, as temperature increases.

It has long been recognized that neutral ion pairs may be responsible for the difference between the overall tracer diffusivity and the charge diffusivity [4]. Hence, we choose ion pairing of the single ions Na^+ and I^- via the reaction

$$Na^+ + I^- \rightleftharpoons (NaI)^0 \tag{1}$$

as a starting point for the analysis of the experimental data. Assuming that beside the neutral pair $(NaI)^0$ higher aggregates may be ignored, the concentration of salt molecules C_s (number density) is the sum of the single-ion concentration ($C_{Na^+} = C_{I^-}$) and the pair concentration C_p expressed by

$$C_s = C_{Na^+} + C_p = C_{I^-} + C_p. \tag{2}$$

For sufficiently fast association and dissociation rates the Na tracer diffusivity D^*_{Na} is composed of the single-ion contribution $\hat{D}_{Na^+}$ and the pair contribution $\hat{D}_p$, i.e.,

$$D^*_{Na} = \hat{D}_{Na^+} + \hat{D}_p = \frac{C_{Na^+} D_{Na^+}}{C_s} + \frac{C_p D_p}{C_s}, \tag{3}$$

where the right-hand side accounts for the probabilities C_{Na^+}/C_s and C_p/C_s that Na occurs as a single-ion and $(NaI)^0$ pair, respectively. In self-explanatory notation, the I tracer diffusivity takes a similar form, i.e.,

$$D^*_I = \hat{D}_{I^-} + \hat{D}_p = \frac{C_{I^-} D_{I^-}}{C_s} + \frac{C_p D_p}{C_s}. \tag{4}$$

The dc conductivity σ_{dc} contains contributions of either ion species but no contribution due to neutral ion pairs. Neglecting correlation effects [5] and using the Nernst-Einstein equation we obtain

$$\sigma_{dc} = \sigma_{Na^+} + \sigma_{I^-} = \frac{e^2}{k_B T}(C_{Na^+} D_{Na^+} + C_{I^-} D_{I^-}), \tag{5}$$

where e denotes elementary charge, k_B Boltzmann's constant, and T temperature. Taking the definition of D_σ used for the conversion of σ_{dc} into diffusivity, it follows that

$$D_\sigma \equiv \frac{\sigma_{dc} k_B T}{C_s e^2} = \hat{D}_{Na^+} + \hat{D}_{I^-}. \tag{6}$$

Equations (3), (4), and (6) contain, apart from the measured diffusivities, three initially unknown "effective"

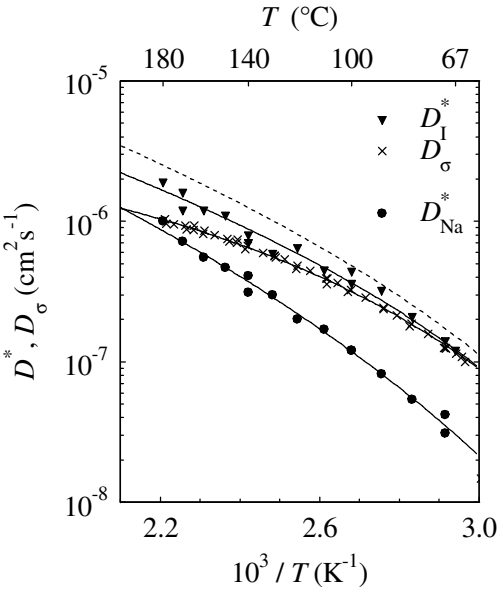

FIG. 2. Tracer diffusion coefficients D^*_{Na} (circles) and D^*_I (triangles) compared to the charge diffusivity D_σ (crosses). Solid lines: fits based on the model described in the text. Dashed lines: sum of D^*_{Na} and D^*_I.

diffusivities $\hat{D}_X$ with $X = Na^+$, I^-, or $p = (NaI)^0$. Solving these equations yields $2\hat{D}_p = D^*_{Na} + D^*_I - D_\sigma$, $2\hat{D}_{Na^+} = D^*_{Na} - D^*_I + D_\sigma$, and $2\hat{D}_{I^-} = -D^*_{Na} + D^*_I + D_\sigma$, which permits us to deduce the temperature dependence of each "hidden" $\hat{D}_X$ parameter from the experimental data. The results of such a preliminary analysis (not shown here) suggested that $\hat{D}_{Na^+}$ and $\hat{D}_{I^-}$ obey a similar VTF behavior, not much different from the temperature dependence of D_σ seen in Fig. 2. In contrast, the $\hat{D}_p$ data so deduced appeared to display a fairly linear shape in the Arrhenius plot, and a stronger variation with temperature. A possible explanation for these observations may involve the pair formation enthalpy ΔH_p which appears through the pair fraction C_p/C_s in $\hat{D}_p$. Specifically, the application of the mass action law to Eq. (1), assuming random mixing of paired and unpaired ions, yields

$$r_p \equiv \frac{C_p}{C_s} = k_p\left(1 - \frac{C_p}{C_s}\right)^2, \tag{7}$$

where the (reduced) ion-pairing reaction constant k_p can be written as

$$k_p = k_{p0}\exp(-\Delta H_p/k_B T). \tag{8}$$

We note that the dimensionless prefactor k_{p0} contains a factor C_s which is a constant within the present context [6]. Solving Eq. (7) provides r_p as a function of temperature, i.e., $r_p = 1 + (1 - \sqrt{1 + 4k_p})/2k_p$ ($\approx k_p - 2k_p^2 + \ldots$), so that the effective diffusivities can be expressed as

$$\begin{aligned} &\hat{D}_p = r_p D_p, \qquad \hat{D}_{Na^+} = (1 - r_p)D_{Na^+}, \\ &\hat{D}_{I^-} = (1 - r_p)D_{I^-}. \end{aligned} \tag{9}$$

Inspired by the results of the preliminary analysis we assume that D_p exhibits the same VTF temperature dependence as D_{Na^+} and D_{I^-}, i.e.,

$$D_X = D^0_X \exp[-B/(T - T_0)] \tag{10}$$

with the initially unknown VTF parameters B and T_0. This assumption bears on the notion that the diffusion of all species is driven by the segmental motion of the polymeric chains.

The above model reveals some analogy to diffusion via paired and unpaired vacancies in alkali halide crystals [7]. It allows us to fit all experimental data simultaneously [cf. Eqs. (3), (4), and (6)], and thus to find estimates for the free parameters B, T_0, $D^0_{Na^+}$, $D^0_{I^-}$, D^0_p, k_{p0}, and ΔH_p. Best fits are displayed in Fig. 2 as solid lines, and the associated parameter values are compiled in Table I. Based on these values, the ion-pairing reaction constant k_p, the true diffusivities D_X, and the effective diffusivities $\hat{D}_X$ can be readily reproduced, as shown in Figs. 3 and 4.

TABLE I. Parameter values and their statistical error obtained from fitting (see text).

B (K)	T_0 (K)	$D^0_{Na^+}$ ($cm^2\,s^{-1}$)	$D^0_{I^-}$ ($cm^2\,s^{-1}$)	D^0_p ($cm^2\,s^{-1}$)	k_{p0}	ΔH_p (eV)
521	225	1.2×10^{-6}	9.7×10^{-6}	8.9×10^{-5}	14	0.19
15%	6%	30%	30%	40%	50%	8%

Figure 2 shows that the present model fits the three sets of experimental data perfectly well. To reduce the statistical uncertainty in the fitting parameters (cf. Table I), the most effective procedure would be the extension of the temperature range. However, amorphous $PEO_{30}NaI$ does not allow for $T < 67\,^\circ C$ because of the crystallization of PEO. On the other hand, for $T > 180\,^\circ C$ the samples were found to be porous and brittle after diffusion annealing and quenching, which is probably due to precipitation of NaI. This "salting out" effect [8,9] may be seen as a consequence of the progressing ion-pair formation with increasing temperature, which is one of the key features emerging from the present work as is discussed next.

In Fig. 3, the ion-pairing reaction constant k_p increases with temperature in agreement with Eq. (8) for an adjusted positive formation energy $\Delta H_p = 0.19$ eV and a corresponding prefactor $k_{p0} = 14$ (Table I). Accordingly r_p varies from ~ 0.02 to ~ 0.1 going from low to high temperature. So at the high end of the T range investigated, ion pairing is becoming substantial. This finding agrees with the results from theoretical [9] and spectroscopic [10] work on PEO-NaI and other polymer electrolytes, respectively. The positive values of ΔH_p and $\Delta S_p (\approx 3k_B)$ associated with k_{p0} imply that the pair formation is entropy driven. The entropy gain may be related to the increase in configurational freedom of the polymer

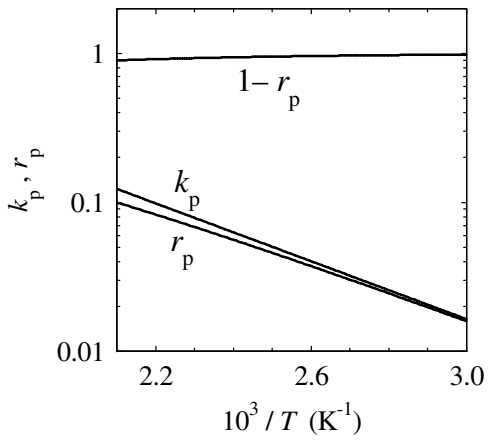

FIG. 3. Temperature dependence of the ion-pairing reaction rate k_p and the $(NaI)^0$ pair fraction r_p as resulting from the model described in the text. The fraction of either single-ion species, $1 - r_p$, is also displayed.

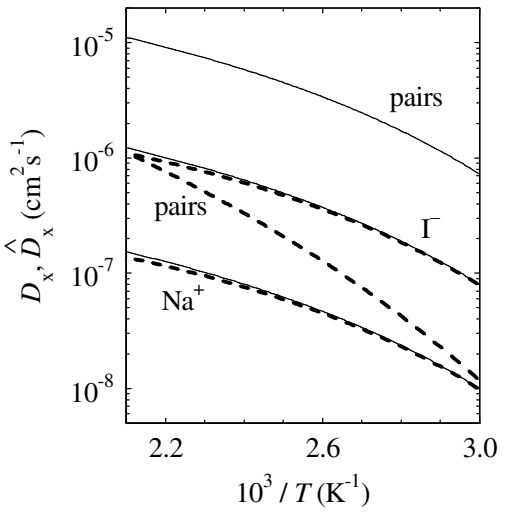

FIG. 4. Diffusivities of single ions (D_{Na^+}, D_{I^-}) and ion pairs (D_p) revealing the same VTF temperature dependence (solid lines: $B = 521K$, $T_0 = 225$ K) and their effective contributions to tracer and charge transport (dashed lines: $\hat{D}_{Na^+} = (1 - r_p)D_{Na^+}$, $\hat{D}_{I^-} = (1 - r_p)D_{I^-}$, $\hat{D}_p = r_p D_p$).

segments due to the decrease of the density of cross-links formed by the oxygen-coordinated cations [10].

Figure 4 displays the true diffusivities D_X of all mobile species and allows for a direct comparison with their effective counterparts $\hat{D}_X$ which include the probability factor C_X/C_s being equal to r_p ($X = p$) or $1 - r_p$ ($X = Na^+, I^-$). It is seen that the three D_X curves run parallel, following the VTF Eq. (10) with $B = 521$ K and $T_0 = 225$ K. The latter value compares to the $\sim$225 K glass transition temperature of $PEO_{30}NaI$ [11] while our B result is not uncommon for PEO-based electrolytes [12]. With the VTF prefactor $D^0_{Na^+} = 1.2 \times 10^{-6}$ cm^2 s^{-1} Na^+ is the slowest mobile species, consistent with its direct bonding to the PEO chains. The larger diffusivity of I^- with $D^0_{I^-}/D^0_{Na^+} \approx 8$ reflects its additional freedom to move about the cations. These features lead to a true cation transference number, $t_+ = D^0_{Na^+}/(D^0_{Na^+} + D^0_{I^-})$, being equal to 0.11 independent of temperature, and thus resolves the conceptional problems related to a ''seemingly'' T-dependent transference number based on D^*_{Na} and D^*_I. The $(NaI)^0$ pair appears to be the fastest among the mobile species ($D^0_p/D^0_{Na^+} = 74$). This indicates that we are dealing with contact pairs in which the Na ion is released from the coordinating oxygen atoms.

Figure 4 further shows that $\hat{D}_{Na^+} \approx D_{Na^+}$ and $\hat{D}_{I^-} \approx D_{I^-}$, whereas $\hat{D}_p$ is much smaller than D_p. Nevertheless, $\hat{D}_p$ distinctly exceeds $\hat{D}_{Na^+}$ in the high-T range, implying that the overall Na transport expressed by D^*_{Na} is dominated by the pair contribution. Altogether, Na diffusion is more strongly influenced by the pair formation than I diffusion. This relates to the circumstance that the slower ionic species can profit more from a small fraction of atoms in a highly mobile state.

In conclusion, this work has contributed to the understanding of ion transport in PEO-NaI polymer electrolytes. It was confirmed that (i) neutral cation-anion pairs contribute to mass transport but not to charge transport and that (ii) the fraction of ion pairs increases with increasing temperature. In addition, strong evidence for the following, so far poorly recognized features was provided: (iii) The diffusivities of the ion pair and the two single ions obey the same VTF temperature dependence. (iv) The magnitude of the diffusivity increases in the order cation, anion, ion pair, which reflects their decreasing degree of coupling to the polymer matrix. (v) The true cation transference number of $\sim$0.1 is T independent and lower than the T-dependent values estimated from the ionic tracer diffusion coefficients. (vi) Cation transport largely takes place in the highly mobile ion-pair configuration.

The authors thank B. Zazoum, H.-D. Wiemhöfer, K. Hagelschur, S. Voss, and A. Imre for helpful cooperation.

*Electronic address: stolwij@uni-muenster.de

[1] N. Boden, S. A. Leng, and I. M. Ward, Solid State Ion. **45**, 261 (1991).
[2] A.V. Chadwick, J. H. Strange, and M. R. Worboys, Solid State Ion. **9–10**, 1155 (1983).
[3] D. Fauteux, M. D. Lupien, and C. D. Robitaille, J. Electrochem. Soc. **134**, 2761 (1987).
[4] P. G. Bruce and C. A. Vincent, Solid State Ionics **40–41**, 607 (1990).
[5] Estimations based on the ion density, $2C_s \approx 10^{20}$ cm^{-3}, and available data for oxide glasses, J. E. Kelly III, J. F. Cordaro, and M. Tomozawa, J. Non-Cryst. Solids **41**, 47 (1980), yield a lower limit for the Haven ratio of 0.8. We checked that the consideration of this ratio in the denominator of Eq. (5) does not change the conclusions of this Letter.
[6] The true reaction constant is k_p/C_s, where $C_s = 8.5 \times 10^{-4}$ mol/cm^3. Similarly, the true prefactor is k_{p0}/C_s.
[7] M. Beniere, M. Chemla, and F. Beniere, J. Phys. Chem. Solids **37**, 525 (1976).
[8] C. K. Chiang, G. T. Davis, C. A. Harding, and J. Aarons, Solid State Ion. **9–10**, 1121 (1983).
[9] V. A. Payne, M. C. Lonergan, M. Forsyth, M. A. Ratner, D. F. Shriver, S.W. de Leeuw, and J.W. Perram, Solid State Ion. **81**, 171 (1995).
[10] S. Schantz, J. Chem. Phys. **94**, 6296 (1991).
[11] M. Minier, C. Berthier, and W. Gorecki, J. Phys. (Paris) **45**, 739 (1984).
[12] D. Bamford, A. Reiche, G. Dlubek, F. Alloin, J.-Y. Sanchez, and M. A. Alam, J. Chem. Phys. **118**, 9420 (2003).